Journal of Earth Science, *Vol. 25*, *No. 4*, *p. 676–688*, *August 2014* *ISSN 1674-487X*
Printed in China
DOI: 10.1007/s12583-014-0457-z

Crustal Stress State and Seismic Hazard along Southwest Segment of the Longmenshan Thrust Belt after Wenchuan Earthquake

Xianghui Qin*, **Chengxuan Tan**, **Qunce Chen**, **Manlu Wu**, **Chengjun Feng**
Institute of Geomechanics, Chinese Academy of Geological Sciences, *Beijing* 100081, *China*; *Key Laboratory of Neotectonic Movement & Geohazard*, *Ministry of Land and Resources*, *Beijing* 100081, *China*

ABSTRACT: The crustal stress and seismic hazard estimation along the southwest segment of the Longmenshan thrust belt after the Wenchuan Earthquake was conducted by hydraulic fracturing for in-situ stress measurements in four boreholes at the Ridi, Wasigou, Dahegou, and Baoxing sites in 2003, 2008, and 2010. The data reveals relatively high crustal stresses in the Kangding region (Ridi, Wasigou, and Dahegou sites) before and after the Wenchuan Earthquake, while the stresses were relatively low in the short time after the earthquake. The crustal stress in the southwest of the Longmenshan thrust belt, especially in the Kangding region, may not have been totally released during the earthquake, and has since increased. Furthermore, the Coulomb failure criterion and Byerlee's law are adopted to analyzed in-situ stress data and its implications for fault activity along the southwest segment. The magnitudes of in-situ stresses are still close to or exceed the expected lower bound for fault activity, revealing that the studied region is likely to be active in the future. From the conclusions drawn from our and other methods, the southwest segment of the Longmenshan thrust belt, especially the Baoxing region, may present a future seismic hazard.
KEY WORDS: Wenchuan Earthquake, Longmenshan thrust belt, in-situ stress measurement, crustal stress state, Coulomb failure criterion, seismic hazard.

0 INTRODUCTION

The occurrence of earthquakes reflects the rapid release of accumulated crustal stress. When the accumulated crustal stress exceeds the ultimate strength of rock mass, an earthquake may be triggered. After the earthquake, the crustal stress will decrease until reaching a new relative equilibrium. Since 1970s, Chinese researchers have attempted to study the occurrence of earthquakes and predict the earthquake migration by analyzing the adjustment of crustal stress before and after large earthquakes (Xie et al., 2005). Evidences related to the adjustment of crustal stress before and after large earthquakes have been obtained for several large earthquakes, such as the 2001 M_s 8.1 Kunlun Earthquake (Liao et al., 2003), the 2008 M_s 8.0 Wenchuan Earthquake (Guo et al., 2009), and the 2011 M_w 7.9 Tohoku-Oki Earthquake, Japan (Lin et al., 2013, 2011). The M_s 8.0 Wenchuan Earthquake was a result of the rapid release of the long-term accumulated crustal stress in the Longmenshan thrust belt caused by the uplift of the Tibetan Plateau. As a result, the crustal stress state in this region will adjust following this large earthquake.

The Wenchuan Earthquake caused major destruction and casualties from fault displacement and direct shaking, and triggered secondary geological effects greatly added to the disaster (Wu et al., 2012; Xu et al., 2012; Qi et al., 2010; Tang et al., 2010). This earthquake formed a surface rupture zone with a length of ~275 km, which started from the epicenter and extended in NE direction (Lin et al., 2009). The earthquake also formed an aftershocks zone with a length of ~330 km, in which over 212 $M_s \geq 4.0$ aftershocks occurred up to July 31th, 2013 according to the data from China Earthquake Data Centre (http://www.csi.ac.cn/Sichuan; http://data.earthquake.cn/index.html). After this large earthquake, researchers studied the geologic background of the large earthquake (Hubbard et al., 2010; Hubbard and Shaw, 2009; Wen et al., 2009; Burchfiel et al., 2008), the recurrence interval (Zhang et al., 2008), the impact of the earthquake on faults in adjacent regions, and the probability of aftershocks (Liu and Shi, 2011; Luo and Liu, 2010; Shao et al., 2010; Zhu and Wen, 2010; Shan et al., 2009; Wan et al., 2009; Parsons et al., 2008). The distributions of the aftershocks varied along the Longmenshan thrust belt. The aftershocks reportedly occurred mostly in the region from Dujiangyan to Qingchuan, with only a few in the southwest segment of the Longmenshan thrust belt, which extends from the Dujiangyan region to the Kangding region (Zheng et al., 2009). Primary results also revealed that this large earthquake effected faults in adjacent region, especially the Xianshuihe fault belt and the Anninghe fault belt, and that more detailed works should be conducted to understand the activity of the southwest segment of the Longmenshan thrust belt (Luo and Liu, 2010; Parsons et al., 2008).

*Corresponding author: qinxiangh03@126.com

Manuscript received August 15, 2013.
Manuscript accepted January 20, 2014.

Qin, X. H., Tan, C. X., Chen, Q. C., et al., 2014. Crustal Stress State and Seismic Hazard along Southwest Segment of the Longmenshan Thrust Belt after Wenchuan Earthquake. *Journal of Earth Science*, 25(4): 676–688. doi:10.1007/s12583-014-0457-z

Since the adjustment of crustal stress is a complicated and longtime process, using data of different methods, such as geology, focal mechanism solution, numerical simulation, and in-situ stress measurements, will be beneficial for understanding the adjustment of tectonic stress before and after the Wenchuan Earthquake and its seismic hazard in the future. In this paper, one site (Baoxing) that is located in the southwest segment of the Longmenshan thrust belt and three sites (Ridi, Wasigou and Dahegou) that are located in the southwest end of this thrust belt are selected to conduct hydraulic fracturing measurements. The data of in-situ stress measured in these four sites in 2003, 2008, and 2010, as well as the results of other methods are adopted to estimate the crustal stress state and seismic hazard in the study region in the future.

1 GEOLOGIC SETTING

As shown in Fig. 1, the study region is located in the intersection of the Bayanhar Block, the Sichuan-Yunnan Block, and the Yangtze Block (Wen et al., 2008; Xu et al., 2008). The study region is in the central segment of the NS-trending seismic belt of China, which is one of China's most active seismic zones, and has caused major destruction and casualties (Deng et al., 1994). Some large historical earthquakes have occurred in this region (see in Fig. 1). The Xianshuihe fault belt, the Longmenshan thrust belt, and the Anninghe fault belt intersect in the study region. The detailed features of these three faults are discussed below.

1.1 Longmenshan Thrust Belt

The Longmenshan thrust belt was a fault-bound depression at a passive continental margin during the Paleozoic. During the Late Triassic, a collision occurred between the Yangtze Block and Qiangtang Massif. This belt was overprinted by younger deformation events, including the Yanshanian Movement and Himalayan Movement (Jin et al., 2010).

Striking ~N40°E, the Longmenshan thrust belt initiates from Luding County, propagates through Dujiangyan City (Guanxian County), Maoxian County (Maowen County), and Beichuan County, Sichuan Province before finally disappearing in Hanzhong City, Shaanxi Province. With over 500 km length and a width of 30–40 km, the Longmenshan thrust belt shows a long history of geologic evolution and complex structures.This active thrust belt consists of three major faults: Wenchuan-Maoxian fault, Beichuan-Yingxiu fault and Guanxian-Anxian fault, from west to east, respectively (Burchfiel et al., 2008; Deng et al., 2003).

Based on the variation of active faults, the Longmenshan thrust belt can be divided into three segments: northeast, southwest, and middle. The northeast segment extends from the Guangyuan region, Sichuan Province to the Ningqiang region, Shaanxi Province. The southwest segment is from the Dujiangyan region to the Kangding region. The middle

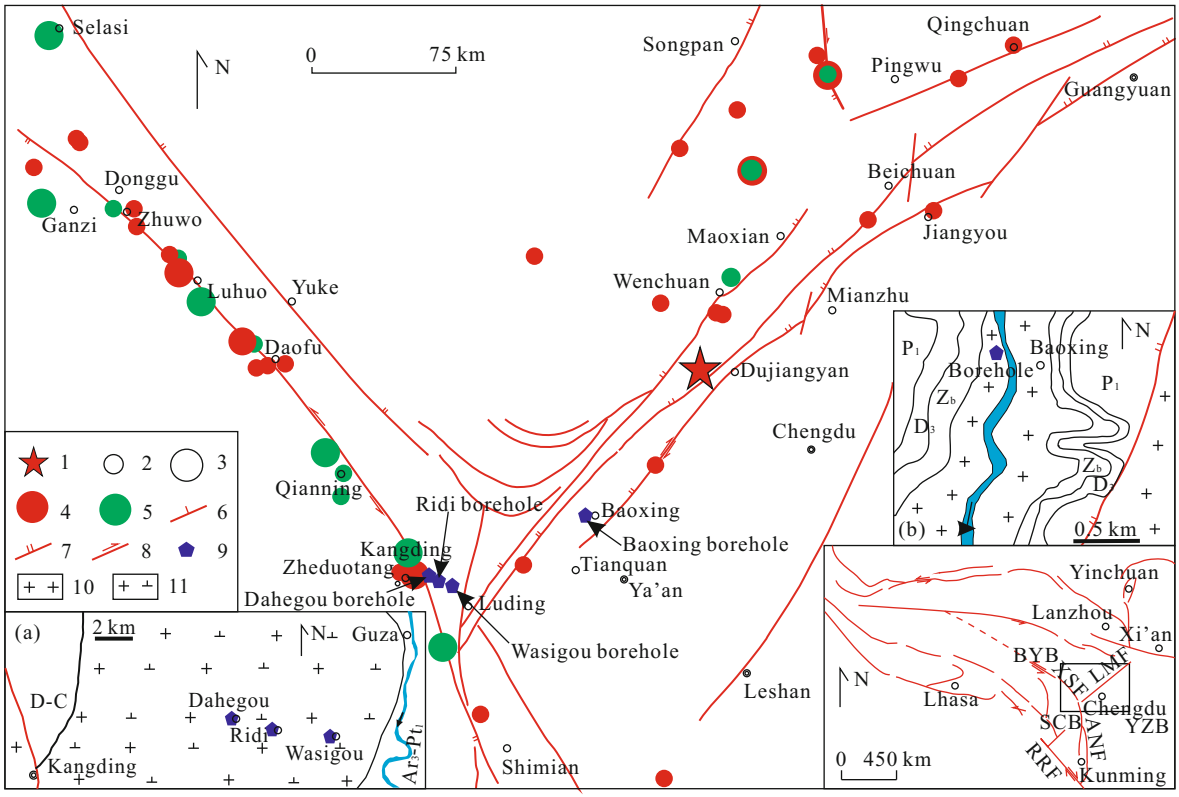

Figure 1. Geologic setting of the study region and locations of in-situ stress measurement sites. (a) Detailed geologic setting of the Ridi, Wasigou, and Dahegou boreholes, and (b) of the Baoxing borehole. 1. The epicenter of the Wenchuan M_s 8.0 Earthquake; 2. M_s 6.0–6.9 earthquakes; 3. M_s 7.0–7.9 earthquakes; 4. earthquakes after 1900; 5. earthquakes before 1900; 6. normal fault; 7. thrust fault; 8. strike-slip fault; 9. in-situ stress measurement boreholes; 10. granite; 11. granodiorite; LMF. Longmenshan fault; XSF. Xianshuihe fault; ANF. Anninghe fault; RRF. Red River fault; BYB. Bayanhar Block; SCB. Sichuan-Yunnan Block; YZB. Yangtze Block.

segment is located between the northeast segment and the southwest segments. Investigations of active fault and GPS monitoring data show that the activities in the middle and southwest segments of Longmenshan thrust belt are relatively strong, while the activity in the northeast segment is relatively weak (Li et al., 2008; Tang et al., 2004; Deng et al., 2003).

The Longmenshan thrust belt also marks the eastern margin zone between the Tibetan Plateau and the Sichuan Basin, which is characterized by rugged mountains with elevations between 580 and 2 300 m, as well as deeply incised valleys and subbasins (Li et al., 2013). The rocks in this region primarily comprise Sinian shale, Cambrian sandstone and siltstone, Ordovician limestone, Silurian slate and phyllite, Devonian limestone, Carboniferous limestone and shale, Permain limestone, and Triassic sandstone and shale. Loose and Quaternary deposits are distributed in the form of terraces and alluvial fans (Tang et al., 2011).

1.2 Xianshuihe Fault Belt

Located insoutheastern region of the Tibetan Plateau, the Xianshuihe fault belt is one of the most active faults in China. It is considered to be the northeast boundary of Sichuan-Yunnan Rhombic Block and the southwest boundary of Bayanhar Block (Deng et al., 2003). The Xiangshuihe fault belt initiates from Ganzi County, extends in ~SE direction, and finally intersects with the Longmenshan thrust belt and the Anninghe fault belt in the Luding region. This fault belt is about ~350 km long and strikes in the NW direction. Based on geometric morphology, the Xiangshuihe fault belt can be divided into two segments, the northwest segment and the southeast segment (Allan, 1991). The geometric morphology of northwest segment, which runs from Ganzi County to Qianning County, is unitary. Alternatively, the southeast segment, which extends from Qianning County to Kangding County, is composed of several subsidiary faults and shows "broom" morphology (Xu et al., 2003). Clusters of large earthquakes have ruptured various segments of the Xianshuihe fault belt since 1700. Seismicity along the Xianshuihe fault belt has been the subject of intensive study in recent years due to its past activity and the more recent Wenchuan Earthquake (Wang et al., 2008; Papadimitriou et al., 2004; Zhang et al., 2003).

1.3 Anninghe Fault Belt

With an ~SE strike direction and a length of 360 km, the Anninghe fault belt shows motion in the form of strike-slip together with some dip-slip. This fault belt, especially the segment from Mianning County to its intersection with the Longmenshan and Xianshuihe fault belts, has shown relatively strong left-lateral motion and seismic activity since the Late Quaternary (Ran et al., 2008; Wen et al., 2008; Deng et al., 2003).

2 METHODS

2.1 Theory

The hydraulic fracturing method of in-situ stress measurement derives from a technique originally developed by the petroleum industry to stimulate oil production by increasing the overall porosity and permeability of rock. As one of the five methods suggested by ISRM (International Society for Rock Mechanics) to estimate stress, hydraulic fracturing in-situ stress measurement has been widely applied in crustal stress estimation and geotechnical engineering. Successful hydraulic fracturing in-situ stress measurements result generally in an estimate of the state of in-situ stress (both magnitudes and directions) in the plane perpendicular to the axis of the borehole. When both the borehole and the induced fractures are nearly vertical, the stress component in the direction of the borehole axis is taken as the principal stress and equals the overburden weight. For a vertical borehole, in-situ stress can be calculated according to the following equations (Haimson and Cornet, 2003; Amadei and Stephansson, 1997)

$$\sigma_h = P_s \tag{1}$$

$$\sigma_H = 3P_s - P_r - P_o \tag{2}$$

$$\sigma_v = \rho g H \tag{3}$$

Here, P_o is pore pressure, which is assumed to equal the hydrostatic pressure (Zoback and Townend, 2001; Barton et al., 1995); P_b is breakdown pressure; P_r is reopening pressure; P_s is shut-in pressure; σ_H is the maximum horizontal principal stress; σ_h is the minimum horizontal principal stress; σ_v is the vertical stress, which is equal to overburden weight. In this article, the mean mass density of rock layer is assumed to be 2.65 g/cm^3.

2.2 Apparatus

The equipment used for the measurements weredeveloped and improved by the authors' institute for hydraulic fracturing stress measurements with 1 000 m test capacity. The single circuit system includes a pressure pump with a maximum pressure to 35 MPa, a set of straddle rubber packers with an interval of 1.00 m and a diameter of 72 mm, a sulfonated rubber impression packer, an orientator including an electronic compass, an automatic data recording system, and an automatic data recording system. The data recording unit is a 12 bite A/D converter; the test data record can be accurately recorded up to 0.01 MPa. Figure 2 shows the photograph of the apparatus used in the in-situ stress measurements mentioned in this paper.

2.3 Procedures

The hydraulic fracturing tests are conducted according to the ISRM suggested procedures for rock stress estimation. The detailed procedure is as followings.

(a) Select test sections that are devoid of fractures or other disturbances.

(b) Leakage hunting of the drilling rodsat pressure of 15–20 MPa.

(c) Lower the straddle packers to the test interval depth through drilling rods.

(d) Pressurize and inflate the two straddle packers to separate the test interval from other sections of the borehole.

(e) Breakdown test. Pump water into the test interval at a faster flowrate until the "breakdown" occurs at the pressure termed "P_b". When a hydraulic tensile fracture is induced on the borehole wall of test interval, pumping is stopped immediately.

(f) Re-opening test. Pump water into the test interval again to raise the pressure until induced tensile fracture is reopened at the pressure termed "P_r". When the induced fracture being

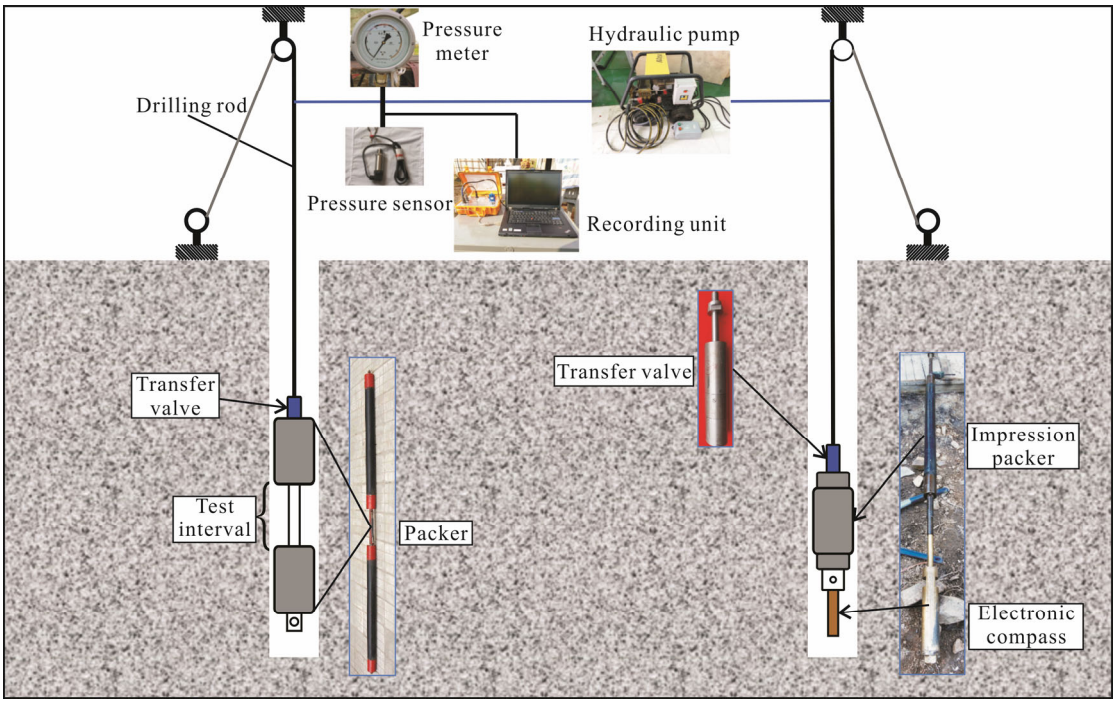

Figure 2. Photograph of the in-situ stress measurement apparatus.

opened, the pump should be stopped to obtain the shut-incurve from which the pressure termed "P_s" (the pressure at which the induced fracture is just merely open and tend to close) can be obtained. The re-opening test should usually be repeated for 3–5 cycles to obtained more accurate records of the shut-in pressure.

(g) Induced fracture impression: An impression packer connected with an electronic compass is positioned at the tested interval, and then pressurized to a pressure higher than the reopening pressure recorded in the re-opening test. The pressure should be kept constant for about 30–60 min to get a distinct geometric copy of the induced tensile fracture. The orientations of σ_H can be calculated according to the copies of induced fractures and the data recorded in the electronic compass.

2.4 Data Processing

The magnitude of in-situ stress can be calculated on the basis of original hydraulic fracturing measurement records, which are pressure-time curves. Figure 3 shows a typical pressure-time curve at a depth of 92.90 m in the Dahegou borehole. To calculate magnitudes of in-situ stress, parameters, such as P_b, P_r, and P_s, should be derived from the field measurements. Several methods have been suggested by ISRM to calculate the P_s, which is the crucial parameter for calculating the magnitudes of stresses. The most commonly adopted methods suggested by ISRM to calculate P_s are dt/dP versus P and dP/dt versus P (Feng et al., 2012; Haimson and Cornet, 2003; Amadei and Stephansson, 1997; Hayashi and Haimson, 1991). In this article, both of these methods are used to calculate the P_s. The dt/dP versus P and dP/dt versus P methods are implemented by software developed by the authors' institute. The average value obtained from these two selected approaches was used to calculate the final shut-in pressure, P_s. The parameters P_b and P_r are also calculated with methods suggested by ISRM.

The orientations of the maximum horizontal stresses are

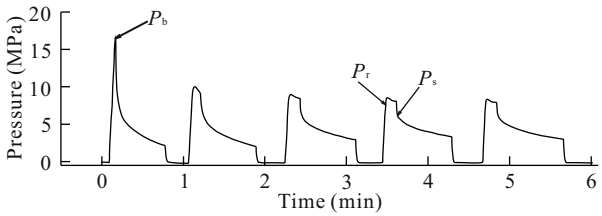

Figure 3. Typical pressure-time curve at 92.90 m depth in the Dahegou borehole.

calculated on the basis of the impression tests of induced fractures and the electronic compass record. The impression tests are conducted with sulfonated rubber packer, which copies the geometry of the induced fractures, and an electronic compass, which records the north line used to calculate the orientation of induced fractures.

3 RESULTS

3.1 In-Situ Stress Measurements

The four boreholes sites, Ridi, Wasigou, Baoxing and Dahegou, are marked in Fig. 1. The primary results of measurements, together with the detailed geologic setting of the four sites are shown and discussed as follows.

(a) Ridi site

The Ridi site is located at the junction region of the Longmenshan thrust belt and the Xianshuihe fault belt. In-situ stress measurements at Ridi site near the Kangding County were conducted in conjunction with the design of the Xiaotiandu hydropower station in 2003. The detailed geologic setting of this site is shown in Fig. 1a. The borehole is located in a small flat piece of land in front of a slope with height less than 100 m. The depth of the Ridi borehole is 230.10 m. The lithology of the Ridi borehole is granodiorite from the Jinning-

Chengjiang Period. The cores extracted from this borehole have high RQD (Rock Quality Designation) value (>91%), and are intact and hard. Results of in-situ stress measurements in the Ridi borehole are summarized in Table 1 (Institute of Crustal Dynamics, 2003).

(b) Wasigou site

Four months after the M_s 8.0 Wenchuan Earthquake, in-situ stress measurements were conducted at Wasigou site, ~5 km away from the Ridi site. The borehole site is in flat land near the main road going from Chengdu City to Lhasa City. The detailed geologic setting of this site is shown in Fig. 1a. The depth of the borehole is 200 m. The lithology is granite of the same geological period as that of the Ridi borehole. The cores in this borehole are relatively intact and hard. Results of the in-situ stress measurements in the Wasigou borehole are summarized in Table 2.

(c) Baoxing site

At approximately the same time that measurements were conducted in the Wasigou borehole, in-situ stress measurements were also conducted at Baoxing site, which is in the vicinity of Baoxing County. The Baoxing site is located in the footwall of the Beichuan-Yingxiu fault and the hanging wall of the Guanxian-Anxian fault. The borehole was located between a slopeless than 200 min height and a road. The detailed geologic setting of this borehole is shown in Fig. 1b; this borehole contains same lithology of granite as in the Ridi and Wasigou boreholes. The borehole depth was 400 m. During drilling, water erupted upon reaching the depth of 160 m, indicating that the water pressure at that depth was relatively high. The high water pressure could be caused by the relatively high level of the crustal stress. Results of in-situ stress measurements in the Baoxing borehole are summarized in Table 3.

Table 1 In-situ stress measurements results in Ridi borehole

Depth (m)	P_o (MPa)	P_b (MPa)	P_r (MPa)	P_s (MPa)	σ_H (MPa)	σ_h (MPa)	σ_v (MPa)	Orientation of σ_H	K_{av}	K_{Hv}	K_{Hh}
158.34	1.58	14.53	10.68	9.98	17.68	9.98	4.20		3.29	4.21	1.77
171.15	1.71	21.27	16.91	13.71	22.51	13.71	4.54		3.99	4.96	1.64
180.15	1.80	14.59	10.19	8.99	14.99	8.99	4.77	N72°E	2.51	3.14	1.67
195.27	1.94	18.74	17.14	13.94	22.74	13.94	5.17		3.55	4.40	1.63
207.35	2.06	22.06	18.06	14.86	24.46	14.86	5.49	N75°E	3.52	4.38	1.65
212.63	2.12	19.72	14.92	14.12	25.32	14.12	5.63	N60°E	3.50	4.50	1.79

$K_{av}=(\sigma_H+\sigma_h)/2\sigma_v$; $K_{Hv}=\sigma_H/\sigma_v$; $K_{Hv}=\sigma_H/\sigma_h$.

Table 2 In-situ stress measurements results in Wasigou borehole

Depth (m)	P_o (MPa)	P_b (MPa)	P_r (MPa)	P_s (MPa)	σ_H (MPa)	σ_h (MPa)	σ_v (MPa)	Orientation of σ_H	K_{av}	K_{Hv}	K_{Hh}
55.00	0.31	4.47	3.27	1.70	1.74	1.70	1.46	N5°E	1.18	1.19	1.02
81.00	0.57	4.66	3.91	2.44	2.84	2.44	2.15	N81°E	1.23	1.32	1.16
94.00	0.70	4.10	3.61	2.52	3.25	2.52	2.49		1.16	1.31	1.29
117.00	0.93	5.03	3.93	2.31	2.46	2.42	3.10		0.79	0.79	1.02
136.00	1.12	9.81	6.12	3.55	3.67	3.55	3.60		1.00	1.02	1.03
143.00	1.19	2.86	2.53	1.95	2.13	1.95	3.79		0.54	0.56	1.09
172.00	1.48	17.32	11.47	5.92	6.41	6.12	4.56		1.37	1.41	1.05
186.00	1.62	10.91	6.89	4.94	6.31	4.94	4.93		1.14	1.28	1.28

Table 3 In-situ stress measurements results in Baoxing borehole

Depth (m)	P_o (MPa)	P_b (MPa)	P_r (MPa)	P_s (MPa)	σ_H (MPa)	σ_h (MPa)	σ_v (MPa)	Orientation of σ_H	K_{av}	K_{Hv}	K_{Hh}
128.00	1.28	6.67	5.96	3.40	3.63	3.53	3.39		1.06	1.07	1.03
156.00	1.56	6.11	5.26	3.44	3.50	3.44	4.13		0.84	0.85	1.02
189.00	1.89	11.71	10.32	7.36	9.87	7.36	5.01	N23°W	1.72	1.97	1.34
219.00	2.19	12.12	8.33	6.45	8.83	6.45	5.80		1.32	1.52	1.37
258.00	2.58	12.53	12.25	9.81	14.60	9.81	6.84		1.78	2.13	1.49
283.00	2.83	16.62	15.76	12.27	18.22	12.27	7.50	N80°W	2.03	2.43	1.48
317.00	3.17	17.29	12.82	11.09	17.28	11.09	8.40	N74°W	1.69	2.06	1.56
354.00	3.54	18.56	18.04	15.75	25.67	15.75	9.38		2.21	2.74	1.63
387.00	3.87	11.86	11.48	10.08	14.89	10.08	10.26		1.22	1.45	1.48

(d) Dahegou site

Two years after the M_s 8.0 Wenchuan Earthquake, in-situ stress measurements were carried out in the Dahegou borehole, which is ~2 km away of the Ridi borehole. The detailed geologic setting of this borehole is also shown in Fig. 1a. The depth of Dahegou borehole, whose lithology is metamorphic sandstone with some coarse-grained granite interbeds, is 200.57 m. With high RQD values (>94%), the cores in this borehole are hard and intact. In addition, disked cores appeared at the depth of 171.02–173.00 m, where the lithology is coarse-grained granite (Fig. 4). Photograph of the disked cores, shown in Fig. 4, reveals that the stress magnitude in this borehole is relatively high. Results of in-situ stress measurements in Dahegou borehole are summarized in Table 4.

3.2 Crustal Stress State

The results of in-situ stress measurements in the four boreholes have been introduced in the previous subsection. The crustal stress state will be estimated in the following section. The crustal stress state includes values of principal stress, orientation of the maximum horizontal stress, and stress regime.

First, the effect of factors such as topography on the results of in-situ stress measurements has been assessed. Since the topography of the Tibetan Plateau changes dramatically and the terrain cutting changes from tens to thousands of meters, the topography would be a prominent factor affecting the

Figure 4. Photograph of disked cores at 171.02–173.00 m depth in the Dahegou borehole.

Table 4 In-situ stress measurements results in Dahegou borehole

Depth (m)	P_o (MPa)	P_b (MPa)	P_r (MPa)	P_s (MPa)	σ_H (MPa)	σ_h (MPa)	σ_v (MPa)	Orientation of σ_H	K_{av}	K_{Hv}	K_{Hh}
86.00	0.65	6.08	3.45	2.52	3.46	2.52	2.28		1.31	1.52	1.37
92.90	0.72	19.39	3.89	3.14	4.81	3.14	2.46	N78°W	1.62	1.96	1.53
103.50	0.83	11.88	4.97	3.80	5.60	3.80	2.74	N9°W	1.72	2.04	1.47
108.86	0.88	14.10	4.01	3.26	4.89	3.26	2.88	N52°E	1.41	1.70	1.50
114.50	0.94	12.17	3.79	3.40	5.47	3.40	3.03	N40°E	1.46	1.81	1.61
121.50	1.01	24.33	19.30	12.83	18.19	12.83	3.22		4.82	5.65	1.42
131.00	1.10	16.46	10.80	7.14	9.52	7.14	3.47		2.40	2.74	1.33
162.50	1.42	24.68	21.73	15.70	23.95	15.70	4.31		4.60	5.56	1.53
171.90	1.51	/	11.42	14.54	30.69	14.54	4.56		4.96	6.73	2.11
185.17	1.64	11.65	11.15	9.80	16.61	9.80	4.91	N26°E	2.69	3.38	1.69

results of in-situ stress measurements. The detailed map of the above four boreholes are shown in Figs. 1a and 1b. Haimson (1980) pointed out that the effective depth of topography was ~30 m in Waterloo, indicating the effect of the topography is mainly focused on the near surface depth. To analyze the effects of topography, Su et al. (2002) collected data on in-situ stresses at the Ertan, Laxiwa, and Xiaowan hydropower stations, all of which are located in sharp valleys. They found that the effective depth of topography was ~30 m at the Ertan site, 1/2–1/3 of the slope height at the Laxiwa site, and 1/4–1/6 of the slope height at the Xiaowan site. Compared with geologic conditions of these hydropower sites, the topographies of the four boreholes in this study are relatively simple. Thus, the effective depth of topography in the four boreholes is expected to be much shallower than in the Su et al.'s sites.

(a) Magnitudes of crustal stress

According to tables showing in-situ stress data in the previous section, we can analyze the magnitudes of the in-situ stresses and the level of the crustal stress in the study regions. With magnitudes of maximum and minimum horizontal stresses ranging from 14.99–25.32 to 8.99–14.86 MPa, respectively, within 200 m depth, the magnitudes of in-situ stresses in the Ridi borehole are some what greater than the expected stresses for that depth and rock type. This indicates a relatively high level of crustal stress. The maximum and minimum horizontal stresses of the Wasigou borehole range from 1.74–6.41 to 1.70–6.12 MPa, respectively, within 200 m depth. This indicates a relatively low level of crustal stress. Based on the depth and rock type, stresses measured in the Baoxing borehole are higher than the expected level; for example, the maximum and minimum horizontal stresses at 354.00 m are 25.67 and 15.75 MPa, respectively. With magnitudes of maximum and minimum horizontal stresses ranging from 3.46–23.95 to 2.52–15.70 MPa, respectively, within 200 m depth, the Dahegou borehole also shows a relatively high level of crustal stress.

To make a detailed estimation of the level of the crustal stress in the study region, the distribution of in-situ stress with depth has been analyzed and plotted in Fig. 5. From Fig. 5, we can see that the values of in-situ stress increase with depth in a relatively linear fashion (Jing et al., 2007; Zhao et al., 2007; Brown and Hoek, 1978). Furthermore, three parameters K_{av}, K_{Hv}, and K_{Hh}, which can characterize the values, are calculated. The parameter K_{av} is the ratio of the mean horizontal stress to the vertical stress, K_{Hv} is the ratio of maximum horizontal stress to vertical stress, and K_{Hh} is the ratio of maximum horizontal stress to minimum horizontal stress. The values of K_{av}, K_{Hv}, and K_{Hh} in the above four boreholes are shown in Tables 1–4. The average values of K_{av}, K_{Hv}, and K_{Hh} are 2.11 (ranging from 0.54 to 4.96), 2.54 (ranging from 0.56 to 6.73), and 1.43 (ranging from 1.02 to 2.11), respectively. The K_{av}, K_{Hv} and K_{Hh} values are consistent with known results (Wang et al., 2012; Yang et al., 2012; Jing et al, 2007; Zhao et al., 2007; Xie et al., 2004; Brown and Hoek, 1978).

(b) Orientation of the maximum horizontal stresses

The orientations of the maximum horizontal stresses (σ_H) in the four boreholes are also shown in Tables 1–4. The preponderant orientation of σ_H at the Ridi site is NNE. Together with data from overcoring, the orientation of σ_H at the Wasigou site can be defined as NE-NNE (Wu et al., 2009). The orientation of σ_H at the Dahegou site can be defined as NE. The orientation of the Baoxing site is NWW, which is consistent with the results of global system position (GPS) and focal mechanism solution results (FMS) (Liu et al., 2012; Yi et al., 2012; Jia et al., 2010).

(c) Stress regime

The stress regime and its implication for faulting scheme in the four sites are estimated according to Anderson's faulting theory (Zoback, 2007; Zoback and Healy, 1992; Jones, 1942). The relation between the three principal stresses is $\sigma_H>\sigma_h>\sigma_v$ in the Ridi, Baoxing, and Dahegou boreholes, while $\sigma_H>\sigma_h\geq\sigma_v$ in the Wasigou borehole. It reveals that all the stress regimes in the study region are conducive to thrust faulting scheme.

(d) Summary

Results of in-situ stress measurements at depths of 150.00–190.00 m in the above four boreholes were selected for detailed analyses. The in-situ stress data reveals that the stress level at Ridi and Dahegou sites exceed that of Wasigou site, indicating that crustal stress in this region decreased during the Wenchuan Earthquake, but quickly increased afterward. Other results indicate that the co-seismic Coulomb stress increased in this junction region, which can even reach the Daofu region (Shan et al., 2013; Zhu and Wen, 2010; Wan and Shen, 2010;

Parsons et al., 2008; Toda et al., 2008). Thus, it can be pointed out that the crustal stress in Kangding region has increased after the Wenchuan Earthquake.

Table 3 reveals that the crustal stress level at the Baoxing site is still high after the large Wenchuan Earthquake. This may indicate that the stress in this segment did not ventor even increase during the earthquake. This effect might be explained by the Baoxing complex as well as the large earthquake, which was thrust type. The results of co-seismic Coulomb stress studies also reveal that the Wenchuan Earthquake increased the co-seismic Coulomb stress in the southwest segment of the Longmenshan thrust belt (Shan et al., 2013; Zhu and Wen, 2010; Wan and Shen, 2010; Parsons et al., 2008; Toda et al., 2008). In terms of these discussions, we can conclude that the Wenchuan

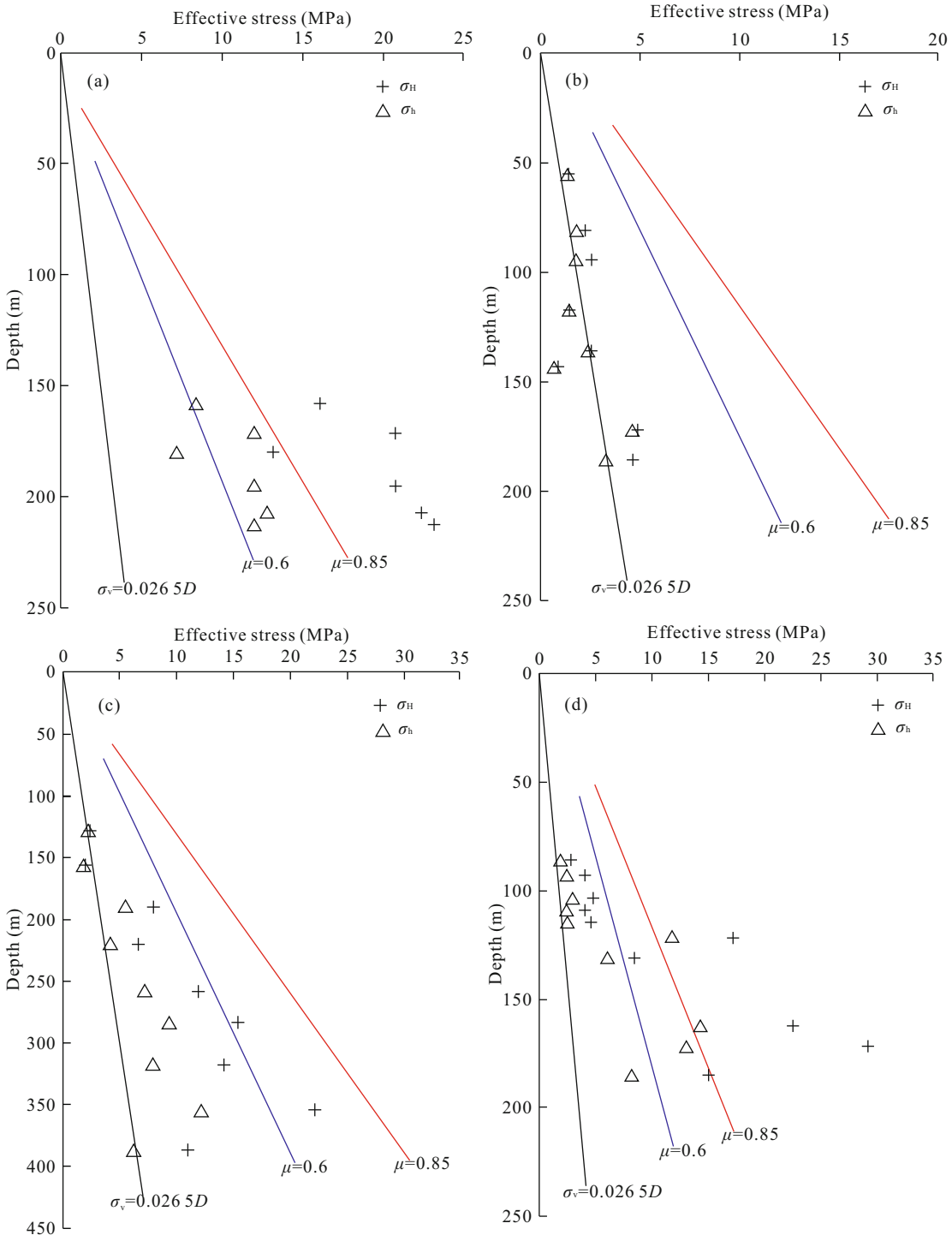

Figure 5. Variation of measured in-situ stress with depth, and the limits of effective stress magnitudes defined by frictional faulting theory at the Ridi (a), Wasigou (b), Baoxing (c), and Dahegou (d) sites. The black solid line represents the magnitudes of effective vertical stress; the blue solid line and red solid line represent the expected lower limit and the upper limit of effective σ_H in the thrust faulting scheme with μ ranging from 0.6–0.85, respectively.

Earthquake has increased the stress level along the southwest segment of the Longmenshan thrust belt, especially in the Baoxing region; additionally, the southwest segment of the Longmenshan thrust belt is a potential seismic hazard region for the future, possibly with large earthquakes (>7.0) (Parsons et al., 2008; Toda et al., 2008).

3.3 Implications for Fault Activity

In-situ stress is an important parameter in understanding the crustal motion, and also has been adopted to assess region crustal stability. This section will focus on the analyses of the implications of the in-situ stress measurements for the fault activity.

The Coulomb criterion indicates that when cohesion is zero and the shear stress τ in fault plane is sufficient to overcome the resistance to slide, $\mu\sigma_n$, frictional sliding will occur on a pre-existing fault plane, and the fault will slip along this plane. The parameter μ is the coefficient of friction for the pre-existing fractures, which can be experimentally determined. The values of σ_1 and σ_3 corresponding to the situation of a critically-oriented fault that is at its frictional limit can be given by the following equation (Jaeger et al., 2007; Zoback, 2007; Zoback and Healy, 1992)

$$\sigma_1/\sigma_3 \leq [(1+\mu^2)^{1/2}+\mu]^2 \quad (4)$$

Here, σ_1 and σ_3 represent the maximum and minimum principal stresses, respectively.

After introducing effective stress, the maximum and minimum effective principal stresses can be defined as (σ_1-P_o) and (σ_3-P_o), respectively. Hence, Eq. (4) can be expressed as following formula

$$(\sigma_1-P_o)/(\sigma_3-P_o) \leq [(1+\mu^2)^{1/2}+\mu]^2 \quad (5)$$

Here, P_o is the pore pressure, which is assumed to be equal to hydrostatic pressure.

If the value of the left of Eq. (5) is lower than that of the right side, the fault will be stable. On the contrary, if the value of the left is equal to or greater than that of the right side, the fault may slip along a suitable plane. The suitable plane, defined by the angle (φ) between the fault-normal and the direction of the maximum principal stress, can be achieved according to following formula

$$\varphi = 1/2(\pi/2+\tan^{-1}\mu) \quad (6)$$

For a different faulting scheme, Eq. (5) should be expressed differently. For the thrust faulting scheme, σ_H and σ_v represent σ_1 and σ_3, respectively. Hence, Eq. (5) for a thrust faulting scheme should be expressed by

$$(\sigma_H-P_o)/(\sigma_v-P_o) \leq [(1+\mu^2)^{1/2}+\mu]^2 \quad (7)$$

To estimate the fault activity with the above formulas, a suitable μ is the key factor. Byerlee (1978) summarized numerous laboratory experiments on a wide variety of faults in different types of rock, noting that the coefficient of friction is within a relatively small range (0.6–1.0) for an extremely wide variety of rock types at elevated effective normal stress (under 100 MPa). Brace and Kohlstedt (1980) has pointed out that the Byerlee's law holds good for upper or lower bound for observed in-situ stress up to 5 km and either pore pressure hydrostatic or subhydrostatic. Based on in-stress measurements in relatively deep boreholes in various parts of the world, Zoback and Townend (2001) pointed out that the ratio of the maximum and minimum effective stress corresponds to a crust in frictional equilibrium with a coefficient friction ranging of 0.6–1.0. Results of the triaxial test in granite, limestone and sandstone in the Three Gorges region in China indicate that the average limit bound can be expressed as $\tau=0.85\sigma_n$ (Li et al., 1993). For this article, thorough understanding of the coefficient of friction of granite and the Longmenshan thrust belt will contribute to the accurate estimation of the fault activity. After summarizing the test results for granite and quartz, Lockner et al. (1986) and Blanpied et al. (1995, 1991) pointed out that the coefficient of friction of these two samples can range of 0.65–0.75, showing only little decrease with the increase water in the sample. When analyzing the mechanics of high-angle reverse fault slip for the Wenchuan Earthquake, Zhou and He (2009) infer that the fault's coefficient of friction and fluid pressure are relatively high, especially in the segment with complexes, such as the Pengguan, Baoxing and Kanding complexes. Sampling along the Beichuan-Yingxiu fault using a triaxial testing machine at conditions corresponding to 2 km depth in the Longmenshan fault belt has been carried out. The steady-state friction coefficient was found to be 0.4 for the natural fault gouge, ~0.6 for the protolith mudstone and sandstone, and 0.6–0.7 for the limestone fault gouge (Zhang and He, 2013; Verberne et al., 2010).

In light of the above discussions, to assess the fault activity along the southwest segment of the Longmenshan thrust belt, the coefficient of friction in Eq. (7) was assumed to be 0.6–0.85. Thus, the lower limit of the coefficient of friction is the same with the widely-used value, while the upper limit is somewhat lower than the value used before.

We analyze the faults activity along the southwest segment of the Longmenshan thrust belt according to the above method. The results of fault activity are plotted in Fig. 5. Figure 5a reveals that the effective stresses in the Ridi borehole exceed the expected upper limit line marked "μ=0.85", revealing that the fault has a good chance of future activity. Figure 5b indicates that the effective stresses in the Wasigou borehole are lower than the expected lower limit line marked "μ=0.6", revealing that the probability for future activity is low or can even be assumed nil. Figure 5c shows that the effective stresses in the Baoxing borehole reach or are nearly equal to the expected lower limit line marked "μ=0.6", indicating that the fault in this region is also likely to be active in the future. The same conclusion can be inferred from other results (Shan et al., 2013; Wan and Shen, 2010; Parsons et al., 2008; Toda et al., 2008). Figure 5d suggests that effective stresses at deep depths in the Dahegou borehole exceed the expected the upper limit line marked with "μ=0.85", revealing that the fault in this region is very likely to exhibit future activity. Because the three boreholes in the Kanding region are relatively shallow, deeper in-situ stress data will contribute to a thorough understanding of the fault activity. Comparing the curves in Fig. 5, it can be pointed out that the southwest segment of Longmenshan thrust belt, especially the southwest end, still stands a good chance of being active in the future, even after the Wenchuan Earthquake.

As mentioned by Byerlee (1978), natural faults always contain clay and minerals such as montmorillonite or vermiculite, which would affect the friction. It has been pointed out that the friction strength increases with effective pressures, and that the frictional strength of shaley rocks is complicated (Zoback, 2007). Carpenter et al. (2009) found that natural serpentinite abutting the San Andreas Fault system at depth exhibited low friction (0.18–0.26). Since the μ of clay gouge fault may be lower, it is possible that frictional failure may be induced under lower stress values than expected, but only if significant quantities of weak clays are present and other conditions, such as the hydrologic setting, are appropriate. This complicated issue needs more detailed study, not only for the Longmenshan thrust belt but also word-wide. According to this discussion, we can suggest that faults in the southwest segment of the Longmenshan thrust belt are likely to be active in the future, even with much lower stress level. Thus, restricted to the measurements of in-situ stress, we suggest that the southwest segment of the Longmenshan thrust belt may be active in the future, and should be marked as a potential seismic hazard region.

4 DISCUSSION

In previous section, we assessed the fault activity along the Longmenshan thrust belt according to in-situ stress data. In addition to these data, other researchers have analyzed the seismic hazard before and after the Wenchuan Earthquake using other methods. Based on regional network seismic data, Yi et al. (2006) preliminarily identified the risky fault segments with potential strong earthquakes occurrence by combing *b*-value spatial distributions and combinations of multiple seismicity parameter values. Yi et al. suggested that the middle-southwest segment of the fault is under high risk of earthquake recurrence. The results of Yi et al. are consistent with conclusion in this article based on the measured in-situ stress data before and after the large earthquake.

Before the M_s 8.0 Wenchuan Earthquake, the seismic activity cycle of the Longmenshan seismic belt was deemed to 300–400 years. After the earthquake, the seismic activity cycle was re-analyzed, and the seismic activity cycle for the strong earthquakes is now deemed to be 2 000–6 000 years (Wen et al., 2011, 2009). Studies also indicate that most of the Longmenshan thrust belt has been in an episode of "quick release of strain energy" since 1879. However, even after the Wenchuan Earthquake, there is still no sufficient evidence to indicate that the episode of "quick release of strain energy" in the eastern boundary of Songpan-Ganzi terrane is or will be over (Wen et al., 2011, 2009). More attention should be paid to the faults in the eastern boundary of Songpan-Ganzi terrane and the adjacent region, as well as faults that have not ruptured in the way of M_s 7.0 earthquake, such as the southern segment of Longmenshan thrust belt and eastern segment of East Kunlun fault belt (i.e., the western region of Wenxian County, Wudu County, and so on) (Wen et al., 2011, 2009; Zhang et al., 2008). Based on the structural setting and three-dimensional modeling of the Longmenshan thrust belt, it was pointed that the large earthquake lowered the stress on the northern part of this fault system, and large earthquakes could still be generated in the southwestern parts of the fault system (Hubbard et al., 2010; Jia et al., 2010; Li et al., 2010; Luo and Liu, 2010; Hubbard and Shaw, 2009). In addition, co-seismic research reveals the increase in the Coulomb stress for the southwest segment of the Longmenshan thrust belt post the Wenchuan Earthquake; additionally, faults such as Ya'an fault has more chance of being active in the future because of the impact of the Wenchuan Earthquake, which is verified by the Lushan Earthquake (Shan et al., 2013; Wan and Shen, 2010; Parsons et al., 2008; Toda et al., 2008). In light of these discussions, we can conclude that the southwest segment of the Longmenshan thrust belt, especially the southwest end of this thrust belt may present a future seismic hazard and need more attention.

5 CONCLUSIONS

In order to thoroughly understand the crustal stress state and seismic hazard along the southwest segment of Longmenshan thrust belt, in-situ stress measurements were conducted by using hydraulic fracturing method; conclusions based on other methods are also adopted and discussed. With these data and analyses, the following conclusions can be drawn.

The in-situ stress data reveal that the stress regimes in the southwest segment of the Longmenshan thrust belt are conducive to the thrust faulting scheme. On the basis of these in-situ stress data, it can be shown that the in-situ stress values along the southwest segment of the Longmenshan thrust belt, especially in the Baoxing, are still relatively high after the Wenchuan Earthquake. This indicates that the stress in this region has increased after the Wenchuan Earthquake.

The levels of in-situ stress in the Kangding region before and after the Wenchuan Earthquake are higher than those during this large earthquake. The crustal stress level in the southwest end of the Longmenshan thrust belt after the Wenchuan Earthquake is close to the pre-earthquake level, revealing that the in-situ stress in this region has been accumulating after the Wenchuan Earthquake. Based on these results, it can be concluded that the strain energy in the southwest segment of the Longmenshan thrust belt may have been partly released during the Wenchuan Earthquake, but has been gradually accumulating ever since.

According to the Coulomb failure criterion and Byerlee's law, the implications of the in-situ stress data for faults activity were estimated. The results reveal that all the magnitudes of in-situ stress in the southwest end of the Longmenshan thrust belt (Kangding region) after the large earthquake exceed the expected upper limit bound inducing fault active. This indicates that this region is still likely to be active in the future after the large Wenchuan Earthquake. The magnitudes of in-situ stress at the Baoxing site after the large earthquake are nearly equal to the expected lower limit bound inducing fault activity, indicating that the fault in this region also stand a good chance of being active in the future. Considered along with the results of other methods in this region, we suggest that the southwest segment of the Longmenshan thrust belt is or will be a seismic hazard region in the future, and more attention should be paid to this region.

On 20th April, 2013, a large M_s 7.0 earthquake occurred in Lushan, Sichuan Province, which is near Baoxing County. This activity verifies the adopted method and conclusions drawn in

this article. In addition, crustal stress monitoring work has been performed in this region. The monitoring of stress data at the Baoxing site implied a good chance for the occurrence of the Lushan Earthquake. The analysis of these monitoring data will help us better understand the adjustment of the crustal stress in this region after these two large earthquakes.

ACKNOWLEDGMENTS

We are grateful to Prof. B C Haimson for critical reading and comments that greatly improved the manuscript. Thanks are due to Prof. Qimei An for his help collecting the in-situ stress data. We also wish to thank the editors and anonymous reviewers for their insightful comments, which improved this article. This study was supported by the Fund of the Institute of Geomechanics (No. DZLXJK201107), the National Scientific Program of China-Experimental Study on the Technique of In-Situ Stress Measurements and Monitoring (No. Sino-Probe-06-03) and the auspice of National Key Basic Project (973) (No. 2008CB425702).

REFERENCES CITED

Allan, C. R., 1991. Field Study of a Highly Active Fault Zone: The Xianshuihe Fault of Southwestern China. *Geol. Soc. Am. Bull.*, 103(9): 1178–1199. doi:10.1130/0016-7606(1991)103

Amadei, B., Stephansson, O., 1997. Rock Stress and Its Measurement. Chapman & Hall, London

Barton, C. A., Zoback, M. D., Moos, D., 1995. Fluid Flow along Potentially Active Faults in Crystalline Rock. *Geology*, 23: 683–686

Blanpied, M. L., Lockner, D. A., Byerlee, J. D., 1991. Fault Stability Inferred from Granite Sliding Experiments at Hydrothennal Conditions. *Geophys. Res. Lett.*, 18(4): 609–612. doi:10.1029/91GL00469

Blanpied, M. L., Lockner, D. A., Byerlee, J. D., 1995. Frictional Slip of Granite at Hydrothermal Conditions. *J. Geophys. Res.* (*Solid Earth*), 100(B7): 13045–13064. doi:10.1029/95JB00862

Brace, W. F., Kohlstedt, D. L., 1980. Limits on Lithospheric Stress Imposed by Laboratory Experiments. *J. Geophys. Res.*, 85(B11): 6248–6252

Brown, E. T., Hoek, E., 1978. Trends in Relationship between Measured In-Situ Stresses and Depth. *Int. J. Rock Mech. Min. Sci. & Geomech. Abstr.*, 15: 211–215

Burchfiel, B. C., Royden, L. H., van der Hilst, R. D., et al., 2008. A Geological and Geophysical Context for the Wenchuan Earthquake of 12 May 2008, Sichuan, People's Republic of China. *GSA Today*, 18(7): 4–11. doi:10.1130/GSATG18A.1

Byerlee, J. D., 1978. Friction of Rocks. *Pure & Applied Geophysics*, 116(4/5): 615–626

Carpenter, B. M., Marone, C., Saffer, D. M., 2009. Frictional Behavior of Materials in the 3D SAFOD Volume. *Geophys. Res. Lett.*, 36: L05320. doi:10.1029/2008gl036660

Deng, Q. D., Chen, S. F., Zhao, X. L., 1994. Tectonics, Seismicity, and Dynamics of the Longmen Shan Mountains and Its Adjacent Region. *Seismology and Geology*, 16(4): 389–403 (in Chinese with English Abstract)

Deng, Q. D., Zhang, P. Z., Ran, Y. K., et al., 2003. Basic Characteristics of Active Tectonics of China. *Science in China Series D*: *Earth Sciences*, 46(4): 356–372

Feng, C. J., Chen, Q. C., Wu, M. L., et al., 2012. Analysis of Hydraulic Fracturing Stress Measurement Data—Discussion of Methods Frequently Used to Determine Instantaneous Shut-in Pressure. *Rock and Soil Mechanics*, 33(7): 2149–2159 (in Chinese with English Abstract)

Guo, Q. L., Wang, C. H., Ma, H. S., et al., 2009. In-Situ Hydr-fracture Stress Measurement before and after the Wenchuan M_s 8 Earthquake of China. *Chinese J. Geophys.*, 52(5): 1395–1401. doi:10.3969/j.issn.0001-5733.2009.05.029

Haimson, B. C., 1980. Near-Surface and Deep Hydrofracturing Stress Measurements in the Waterloo Quartzite. *Int. J. Rock Mech. Min. Sci.*, 17: 81–88

Haimson, B. C., Cornet, F. H., 2003. ISRM Suggested Methods for Rock Stress Estimation-Part 3: Hydraulic Fracturing (HF) and/or Hydraulic Testing of Pre-Existing Fractures (HTPF). *Int. J. Rock Mech. Min. Sci.*, 40: 1011–1020. doi:10.1016/j.ijrmms.2003.08.002

Hayashi, K., Haimson, B. C., 1991. Characteristics of Shut-In Curves in Hydraulic Fracturing Stress Measurements and Determination of In Situ Minimum Compressive Stress. *J. Geophys. Res.*, 96(B11): 18311–18321

Hubbard, J., Shaw, J. H., 2009. Uplift of the Longmen Shan and Tibetan Plateau, and the 2008 Wenchuan (M=7.9) Earthquake. *Nature*, 458: 194–497. doi:10.1038/nature07837

Hubbard, J., Shaw, J. H., Klinger, Y., 2010. Structural Setting of the 2008 M_w 7.9 Wenchuan, China, Earthquake. *Bull. Seismol. Soc. Am.*, 100(5B): 2713–2735. doi:10.1785/0120090341

Institute of Crustal Dynamics, 2003. Hydro-Fracture In-Situ Stress Measurements in ZK1 Borehole in Xiaotiandu Hydropower Station. Seismological Press, Beijing (in Chinese)

Jaeger, J. C., Cook, N. G. W., Zimmerman, R. W., 2007. Fundamentals of Rock Mechanics (4th Edition). Blackwell Publishing, Oxford

Jia, D., Li, Y. Q., Lin, A. M., et al., 2010. Structural Model of 2008 M_w 7.9 Wenchuan Earthquake in the Rejuvenated Longmen Shan Thrust Belt, China. *Tectonophysics*, 491: 174–184. doi:10.1016/j.tecto.2009.08040

Jin, W. Z., Tang, L. J., Yang, K. M., et al., 2010. Segment of the Longmen Mountains Thrust Belt, Western Sichuan Foreland Basin, SW China. *Tectonophysics*, 485: 107–121. doi:10.1016/j.tecto.2009.12.007

Jing, F., Sheng, Q., Zhang, Y. H., 2007. Research on Distribution Rule of Shallow Crustal Geostress in China Mainland. *Chin. J. Rock Mech. Eng.*, 26(10): 2057–2062 (in Chinese with English Abstract)

Jones, O. T., 1942. Faulting and Dyke Formation-The Dynamics of Faulting and Dyke Formation: With Application to Britain, *Nature*, 3789: 651–652

Li, F. Q., Zhang, B. C., Su, K. Z., 1993. Reservoir Induced Earthquake Risk in the Yangtze Gorges Dam Area. Seismological Press, Beijing (in Chinese)

Li, H. B., Wang, H., Xu, Z. Q., et al., 2013. Characteristics of the Fault-Related Rocks, Fault Zone and the Principal Slip Zone in the Wenchuan Earthquake Scientific Drilling Project Hole-1 (WSFD-1). *Tectonophysics*, 584: 23–42.

doi:10.1016/j.tecto.2012.08.021

Li, Y. Q., Jia, D., Shaw, J. H., et al., 2010. Structural Interpretation of the Co-Seismic Faults of the Wenchuan Earthquake: Three-Dimensional Modeling of the Longmen Shan Fold-and-Thrust Belt. *J. Geophys. Res.*, 115. doi:10.1029/2009JB006824

Li, Z. W., Liu, S. G., Chen, H. D., et al., 2008. Structural Segmentation and Zonation and Differential across and along the Longmen Thrust Belt, West Sichuan, China. *Journal of Chengdu University of Technology* (*Science & Technology Edition*), 35(4): 440–453 (in Chinese with English Abstract)

Liao, C. T., Zhang, C. S., Wu, M. L., et al., 2003. Stress Change near the Kunlun Fault before and after the M_S 8.1 Kunlun Earthquake. *Geophys. Res. Lett.*, 27(20). doi:10.1029/2003GL018106

Lin, A. M., Ren, Z. K., Jia, D., et al., 2009. Co-Seismic Thrusting Rupture and Slip Distribution Produced by the 2008 M_W 7.9 Wenchuan Earthquake, China. *Tectonophysics*, 471(3/4): 203–215. doi:10.1016/j.tecto.2009.02.014

Lin, W. R., Saito, S., Sanada, Y., et al., 2011. Principal Horizontal Stress Orientations Prior to the 2011 M_W 9.0 Tohoku-Oki, Japan, Earthquake in Its Source Area. *Geophys. Res. Lett.*, 38: L00G10. doi:10.1029/2011GL049097

Lin, W. R., Conin, M., Moore, C., et al., 2013. Stress State in the Largest Displacement Area of the 2011 Tohoku-Oki Earthquake. *Science*, 339: 687–690. doi:10.1126/science.129379

Liu, B. Y., Shi B. P., 2011. The State of Stress of the M_S 8.0 Wenchuan Earthquake Faulting and Its Implication to the Aftershock Hazard. *Chinese J. Geophys.*, 54(4): 1002–1009. doi:10.3969/j.issn.0001-5733.2011.04.015

Liu, J., Xiong, T. Y., Zhao, Y., et al., 2012. Kinematic Characteristics of Longmenshan Active Fault Zone and Its Tectonic Implication. *J. Jilin Univ.* (*Earth Sci.*), 42(S2), 320–330 (in Chinese with English Abstract)

Lockner, D. A., Summers, R., Byerlee, J. D., 1986. Effects of Temperature and Sliding Rate on Frictional Strength of Granite. *Pure Applied Geophysics*, 124: 445–469

Luo, G., Liu, M., 2010. Stress Evolution and Fault Interactions before and after the 2008 Great Wenchuan Earthquake, *Tectonophysics*, 491: 127–140. doi:10.1016/j.tecto.2009.12.019

Papadimitriou, E., Wen, X. Z., Karakostas, V., et al., 2004. Earthquake Triggering along the Xianshuihe Fault Zone of Western Sichuan, China. *Pure and Applied Geophysics*, 161(8): 1683–1707. doi:10.1007/s00024-003-2471-4

Parsons, T., Ji, C., Kirby, E., 2008. Stress Changes from the 2008 Wenchuan Earthquake and Increased Hazard in the Sichuan Basin. *Nature*, 454(7203): 509–510. doi:10.1038/nature07177

Qi, S. W., Xu, Q., Lan, H. X., et al., 2010. Spatial Distribution Analysis of Landslides Triggered by 2008.5.12 Wenchuan Earthquake, China. *Engineering Geology*, 116: 95–108. doi:10.1016/j.enggeo.2010.07.011

Ran, Y. K., Chen, L. C., Cheng, J. W., et al., 2008. Late Quaternary Surface Deformation and Rupture Behavior of Strong Earthquake on the Segment North of Mianning of the Anninghe Fault. *Science in China Series D*: *Earth Sciences*, 51(9): 1224–1237. doi:10.1007/s11430-008-0104-6

Shan, B., Xiong, X., Zheng, Y., et al., 2009. Stress Changes on Major Faults Caused by M_W 7.9 Wenchuan Earthquake, May 12, 2008. *Science in China Series D*: *Earth Sciences*, 52(5): 593–601. doi:10.1007/s11430-009-0060-9

Shan, B., Xiong, X., Wang, R. J., et al., 2013. Coulomb Stress Evolution along Xianshuihe-Xiaojiang Fault System since 1713 and Its Interaction with Wenchuan Earthquake, May 12, 2008. *Earth Planet. Sci. Lett.*, 377/378: 199–210. doi:10.1016/j.epsl.2013.06.044

Shao, Z. G., Zhou, L. Q., Jiang, C. S., et al., 2010. The Impact of Wenchuan M_S 8.0 Earthquake on the Seismic Activity of Surrounding Faults. *Chinese J. Geophys.*, 53(8): 1784–1795. doi:10.3969/j.issn.001-5733.2010.08.04

Su, S. R., Huang, R. Q., Wang, S. T., 2002. Effect of Faults on In Situ Stress and Application in Engineering. Science Press, Beijing. 21–30 (in Chinese)

Tang, C., Zhu, J., Qi, X., et al., 2011. Landslides Induced by the Wenchuan Earthquake and the Subsequent Strong Rainfall Event: A Case Study in the Beichuan Area of China. *Engineering Geology*, (122): 22–33. doi:10.1016/j.enggeo.2011.03.013

Tang, H. M., Jia, H. B., Hu, X. L., et al., 2010. Characteristics of Landslides Induced by the Great Wenchuan Earthquake. *Journal of Earth Science*, 21(1): 104–113. doi:10.1007/s12583-010-0008-1

Tang, W. Q., Liu, Y. P., Chen, Z. L., et al., 2004. GPS Study on Longmenshan Fracture Belt Zone. *Journal of Geodesy and Geodynamics*, 24(3): 57–59 (in Chinese with English Abstract)

Toda, S. J., Lin, J., Meghraoui, M., et al., 2008. 12 May 2008 *M*=7.9 Wenchuan, China, Earthquake Calculated to Increase Failure Stress and Seismicity Rate on Three Major Fault Systems. *Geophys. Res. Lett.*, 35(17). doi:10.1029/2008GL034903

Verberne, B. A., He, C. R., Spiers, C. J., 2010. Frictional Properties of Sedimentary Rocks and Natural Fault Gouge from the Longmen Shan Fault Zone, Sichuan, China. *Bull. Seismol. Soc. Am.*, 100: 2767–2790. doi:10.1785/0120090287

Wan, Y. G., Shen, Z. K., Sheng, S. Z., et al., 2009. The Influence of 2008 Wenchuan Earthquake on Surrounding Faults. *Acta Seismologica Sinica*, 31(2): 128–139 (in Chinese with English Abstract)

Wan, Y. G., Shen, Z. K., 2010. Static Coulomb Stress Changes on Faults Caused by the 2008 M_W 7.9 Wenchuan, China Earthquake. *Tectonophysics*, 491(1–4): 105–118. doi:10.1016/j.tecto.2010.03.017

Wang, H., Liu, J., Shi, Y. L., et al., 2008. Dynamic Modeling of Interactions between Big Earthquakes along the Xianshuihe Fault Zone. *Science in China Series D*: *Earth Sciences*, 51(10): 1388–1400. doi:10.1007/s11430-008-0110-8

Wang, Y. H., Cui, X. F., Hu, X. P., et al., 2012. Study on the Stress State in Upper Crust of China Mainland Based on In-Situ Stress Measurements. *Chinese J. Geophys.*, 55(9): 3016–3027. doi:10.6038/j.issn.0001-5733.2012.09.020 (in Chinese with English Abstract)

Wen, X. Z., Ma, S. L., Xu, X. W., et al., 2008. Historical Pattern and Behavior of Earthquake Ruptures along the Eastern Boundary of the Sichuan-Yunnan-Block, Southwestern

China. *Physics of the Earth and Planetary Interiors*, 168(1/2): 16–36. doi:10.1016/j.pepi.2008.04.013

Wen, X. Z., Zhang, P. Z., Du, F., et al., 2009. The Background of Historical and Modern Seismic Activities of Occurrence of the M_S 8.0 Wenchuan, Sichuan Earthquake. *Chinese J. Geophys.*, 52(2): 444–454 (in Chinese with English Abstract)

Wen, X. Z., Du, F., Zhang, P. Z., et al., 2011. Correlation of Major Earthquake Sequences on the Northern and Eastern Boundaries of the Bayan Har Block, and Its Relation to the 2008 Wenchuan Earthquake. *Chinese J. Geophys.*, 54(3): 706–716. doi:10.3969/j.issn.0001-5733.2011.03.010 (in Chinese with English Abstract)

Wu, M. L., Zhang, Y. Q., Liao, C. T., et al., 2009. Preliminary Results of In-Situ Stress Measurements along the Longmenshan Fault Zone after the Wenchuan M_S 8.0 Earthquake. *Acta Geologica Sinica*, 83(4): 746−753

Wu, Z. H., Barosh, P. J., Zhang, Z. C., et al., 2012. Effect from the Wenchuan Earthquake and Seismic Hazard in the Longmenshan Mountains at the Eastern Margin of the Tibetan Plateau. *Engineering Geology*, (143/144): 28–36. doi:10.1016/j.enggeo.2012.06.006

Xie, F. R., Cui, X. F., Zhao, J. T., 2004. Regional Division of the Recent Tectonic Stress Field in China and Adjacent Area. *Chinese J. Geophys.*, 47(4): 654–662 (in Chinese with English Abstract)

Xie, F. R., Qiu, Z. H., Wang, Y., et al., 2005. Earth Stress Observation and Earthquake Prediction. *Recent Developments in World Seismology*, 317(5): 54–59 (in Chinese with English Abstract)

Xu, C., Xu, X. W., Dai, F. C., et al., 2012. Landslide Hazard Mapping Using GIS and Weight of Evidence Model in Qingshui River Watershed of 2008 Wenchuan Earthquake Struck Region. *Journal of Earth Science*, 23(1): 97–120. doi:10.1007/s12583-012-0236-7

Xu, X. W., Wen, X. Z., Zhen, R. Z., et al., 2003, Pattern of Latest Tectonic Motion and Its Dynamics for Active Blocks in Sichuan-Yunnan Region, China. *Science in China Series D*: *Earth Sciences*, 46(Suppl.): 210–226. doi:10.1360/03dz0017

Xu, Z. Q., Ji, S. C., Li, H. B., et al., 2008. Uplift of the Longmen Shan Range and the Wenchuan Earthquake. *Episodes*, 31(3): 291–301

Yang, S. X., Yao, R., Cui, X. F., 2012. Analysis of the Characteristics of Measured Stress in Chinese Mainland and Its Active Block and North-South Seismic Belt. *Chinese J. Geophys.*, 55(12): 4207–4217. doi:10.6038/j.issn.0001-5733.2012.12.032 (in Chinese with English Abstract)

Yi, G. X., Wen, X. Z., Wang, S. W., et al., 2006. Study on Fault Sliding Behaviors and Strong Earthquake Risk of the Longmenshan-Minshan Fault Zones from Current Seismicity Parameters. *Earthquake Research in China*, 22(2): 117–125 (in Chinese with English Abstract)

Yi, G. X., Long, F., Zhang, Z. W., 2012. Spatial and Temporal Variation of Focal Mechanisms for Aftershocks of the 2008 M_S 8.0 Wenchuan Earthquake. *Chinese J. Geophys.*, 55(4): 1213–1227. doi:10.6038/j.issn.0001-5733.2012.04.017 (in Chinese with English Abstract)

Zhang, L., He, C. R., 2013, Frictional Properties of Natural Gouges from Longmenshan Fault Zone Ruptured during the Wenchuan M_W 7.9 Earthquake. *Tectonophysics*, 594: 149–164. doi:10.1016/j.tecto.2013.03.030

Zhang, P. Z., Xu, X. W., Wen, X. Z., et al., 2008. Slip Rates and Recurrence Intervals of the Longmenshan Active Fault Zone and Tectonic Implications for the Mechanism of the May 12 Wenchuan Earthquake, 2008, Sichuan, China. *Chinese J. Geophys.*, 51(4): 1066–1073 (in Chinese with English Abstract)

Zhang, Q. W., Zhang, P. Z., Wang, C., et al., 2003. Earthquake Triggering and Delaying Caused by Fault Interaction on Xianshuihe Fault Belt, Southwestern China. *Acta Seismologica Sinica*, 25(2): 156–165

Zhao, D. A., Chen, Z. M., Cai, X. L., et al., 2007. Analysis of Distribution Rule of Geostress in China. *Chin. J. Rock Mech. Eng.*, 26(6): 1265–1271 (in Chinese with English Abstract)

Zheng, Y., Ma, H., Lü, J., et al., 2009. Source Mechanism of Strong Aftershocks (M_S≥5.6) the 2008/05/12 Wenchuan Earthquake and the Implication for Seismotectonics. *Science in China Series D*: *Earth Sciences*, 52(5): 739–753. doi:10.1007/s11430-009-0074-3

Zhou, Y. S., He, C. R., 2009. The Rheological Structures of Crustal and Mechanics of High-Angle Reverse Fault Slip for Wenchuan M_S 8.0 Earthquake. *Chinese J. Geophys.*, 52(2): 474–484 (in Chinese with English Abstract)

Zhu, H., Wen, X. Z., 2010. Static Stress Triggering Effects Related with M_S 8.0 Wenchuan Earthquake. *Journal of Earth Science*, 21(1): 32–41. doi:10.1007/s12583-010-0001-8

Zoback, M. D., Healy, J. H., 1992. In-Situ Stress Measurements to 3.5 km Depth in the Cajon Pass Scientific Research Borehole: Implications for the Mechanics of Crustal Faulting. *J. Geophys. Res.*, 97(B4): 5039–5057

Zoback, M. D., Townend, J., 2001. Implications of the Hydrostatic Pore Pressures and High Crustal Strength for the Deformation of Intraplate Lithosphere. *Tectonophysics*, 336(1–4): 19–30

Zoback, M. D., 2007. Reservoir Geomechanics. Cambridge University Press, Cambridge. 123–139